Operation of a Ramsey-CPT microcell atomic clock with driving current-based power modulation of a VCSEL

C. M. Rivera-Aguilar, M. Callejo, A. Mursa, C. Carlé, R. Vicarini, M. Abdel Hafiz, J-M. Friedt, N. Passilly, and R. Boudot

FEMTO-ST, CNRS, Université de Franche-Comté, ENSMM, Besançon, France

(*Electronic mail: rodolphe.boudot@femto-st.fr)

(Dated: 11 March 2024)

We report on the operation of a coherent population trapping (CPT) microcell atomic clock using a pulsed Ramsey-like interrogation. The Ramsey-CPT sequence, defined by two-step optical pulses separated by a free-evolution dark time, is produced by switching on and off the output power of a low-power vertical-cavity surface-emitting laser (VCSEL), through direct modulation of its driving current. High-contrast and narrow Ramsey-CPT fringes are detected without the use of any external optical modulator stage. We demonstrate closed-loop operation of the clock based on high speed digital signal processing implemented in a FPGA board. The clock short-term fractional frequency stability is $1.3 \times 10^{-10} \ \tau^{-1/2}$ until 2000 s. A power light-shift coefficient of $8 \times 10^{-11}/\mu$ W, in relative value, is obtained for a dark time of 150 μ s. This value is about 10 times lower than in the continuous regime. These results show the feasibility of fully-integrated atomic clocks based on Ramsey spectroscopy, that could provide enhanced long-term stability.

Miniaturized microwave atomic clocks based on coherent population trapping (CPT) have met with remarkable success by offering fractional frequency stability in the low 10⁻¹¹ range at 1 day integration time in a low size-weight and power (SWaP) budget¹. These clocks, that rely on the interaction of a hot alkali vapor confined in a microfabricated cell²⁻⁵ with an optically-carried microwave interrogation field obtained by direct current modulation of a vertical-cavity surface-emitting laser (VCSEL)⁶, offer instabilities at 1 day 100 times smaller than their quartz-crystal oscillators counterparts, while providing much shorter warm-up times. These unrivaled features have motivated the deployment of chip-scale atomic clocks (CSACs) in underwater sensing, precise navigation and timing (PNT) systems or secure communications.

A key performance criteria of a CSAC is its long-term stability. The latter can be degraded by several mechanisms, among which light-shifts are recognized as a major contributor⁷. In most CSACs, atoms interact continuously with the probing light field. In this continuous-wave (CW) interrogation regime, numerous methods have been proposed for light-shift mitigation. These methods usually rely on the active stabilization of a finely-tuned microwave power that cancels, at the first order, the dependence of the clock frequency to laser power⁷⁻¹¹, compensation of the laser frequency aging using smart algorithms that control the VCSEL dc current-temperature couple¹², or the adjustment of the cell temperature to a specific setpoint¹³. Interrogation sequences that rely on the extraction of atomic information from two successive light-shifted clock frequencies, obtained at two different laser-power values¹⁴, were also demonstrated on microcell CPT clocks¹⁵.

An alternative approach for light-shift mitigation in CPT clocks is to use Ramsey spectroscopy. In this case, atoms interact with a sequence of optical CPT pulses separated by a free-evolution dark time T. Widely used in high-performance vapor cell¹⁶ and cold atom clocks^{17,18}, Ramsey-CPT spectroscopy has been studied in microfabricated cells^{19,20}. More sophisticated sequences, such as symmetric auto-balanced Ramsey (SABR) spectroscopy^{21,22}, have also been adapted

in microcell CPT clocks for further reduction of light-shift coefficients 23 . Using a Cs-Ne microcell built with aluminosilicate glass (ASG) windows, a pulsed SABR-CPT clock with a frequency stability of 1.4×10^{-12} at 1 day was demonstrated 24 .

In the above-mentioned experiments, the pulsed Ramsey-CPT sequence was produced thanks to an external acoustooptic modulator (AOM). Yet, the AOM component is far too bulky and power consuming to be used in a CSAC. Two main approaches, using direct modulation of the VCSEL current, have been proposed to address this issue. The first one consists on switching on and off the microwave power that modulates the VCSEL current²⁵. A drawback of this method is the persistence of residual carrier light during the free-evolution time T, which might create excess light-shifts. The second option is to directly modulate the VCSEL bias current in order to switch on and off the laser output power. In this case, no light perturbs the atomic transitions during the free-evolution time. However, the sudden change in bias current induces a change in the junction temperature of the VCSEL, that results in a gradual evolution of its wavelength. The time needed to reach a new thermal equilibrium at the atom wavelength, and measure a useful atomic signal, is then too long.

Employing a sequence made of two-step pulses, the first step being shorter and more intense, was shown to effectively reduce the duration required to achieve the wavelength desired for observation²⁶. During the initial step, the VCSEL junction quickly heats up. A delay of 10-20 μ s is then enough to reach the optical resonance wavelength, for a brief duration. The second lower current step allows the VCSEL junction to cool down and reach thermal equilibrium, such that the absorption line wavelength is crossed once more, and a steady CPT state is obtained. Several light-shift studies have been reported with this technique^{26–29}. However, all of these studies were performed in cm-scale cells, in which long CPT coherence lifetimes of a few ms can be achieved. Also, no clock frequency Allan deviation was reported.

The two-step pulse Ramsey-CPT sequence explored in Refs^{26–29} has never been demonstrated in a microfabricated

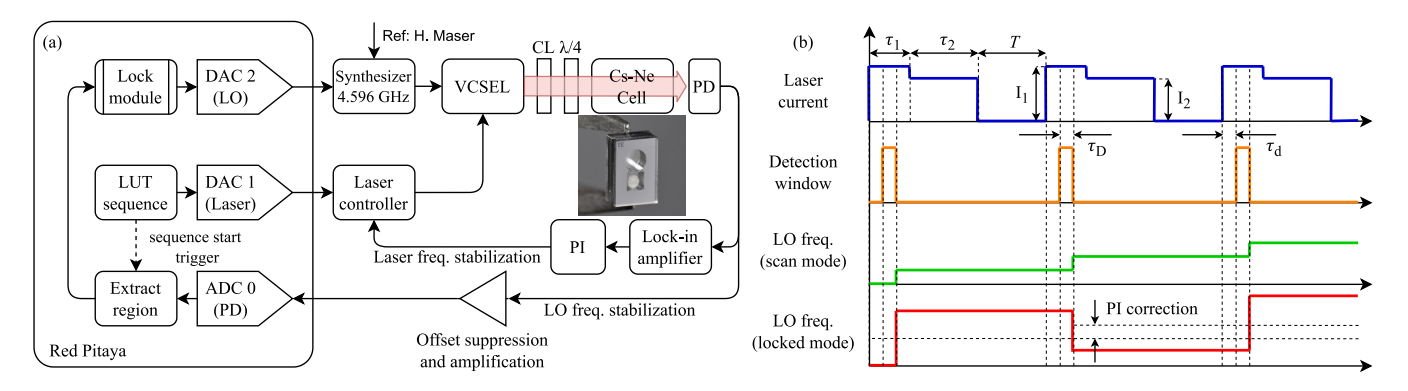


FIG. 1: (a) Experimental setup. CL: collimation lens. PD: photodiode. DAC: digital-to-analog converter. ADC: analog-to-digital converter. LUT: Look-Up table. LO: local oscillator. PI: proportional-integral controller. The inset shows a photograph of the microfabricated cell. (b) Ramsey sequence with two-step pulses separated by a free-evolution dark time T. Timing $(\tau_1, \tau_2, \tau_D, \tau_d)$ and current $(I_1 \text{ and } I_2)$ parameters are discussed in the text.

cell, similar to those used in CSACs. In a mm-scale cell, the reduced CPT coherence lifetime imposes shorter timescales on the light pulse sequence. Also, the use of higher buffer gas pressures and alkali densities increase the mixing between excited states. The implementation of high-speed and agile digital electronics is therefore of particular importance in a microcell experiment for acquiring, averaging and processing the atomic signal within a time frame of a few microseconds.

In this paper, we demonstrate, using a two-step pulse sequence²⁶, the operation of a Ramsey-CPT microcell atomic clock with driving current-based power modulation of a VC-SEL. No external optical modulation stage is used. We report the detection of high-contrast and narrow Ramsey-CPT fringes in a Cs-Ne micromachined cell and study the impact of the dark time T on the central fringe's amplitude and linewidth. A clock short-term frequency stability of $1.3 \times 10^{-10} \tau^{-1/2}$ until 2000 s is obtained. For $T = 150 \mu s$, the clock frequency dependence to laser power variations is measured to be about 10 times smaller than the one obtained in the CW regime. These results confirm the interest of this approach for the development of pulsed microcell CSACs, with low light-shift sensitivity and improved long-term stability.

Figure 1(a) shows the CPT clock architecture. This setup was specifically built for this work. We use a VCSEL tuned on the Cs D_1 line at 895 nm³⁰. In continuous operation, the laser frequency is tuned onto the Cs line for a temperature of 77°C and a dc current of 2 mA. The VCSEL is modulated through a bias tee by a 4.596 GHz signal, provided by a commercial microwave synthesizer, used as the local oscillator (LO). The latter is referenced to a hydrogen maser for frequency shift and stability measurements. In closed loop operation, we refer to the synthesizer output value as the clock frequency. The output laser beam is collimated with a lens and circularly polarized with a quarter-wave plate. A neutral density filter (NDF) allows for changing the laser power P_l at the cell input, measured through a 50-50 beam splitter (not shown on Fig. 1). The 2 mm diameter beam illuminates a Cs vapor microfabricated cell^{31,32} filled with about 63 Torr of Ne buffer gas. The atom-light interaction takes place in a 2

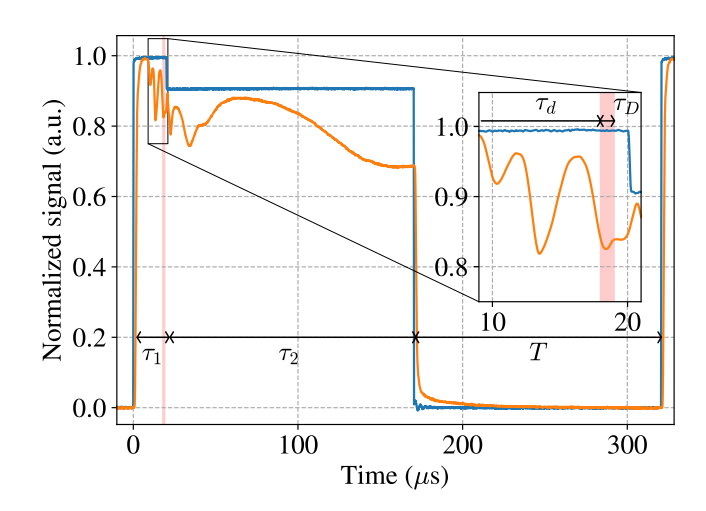


FIG. 2: Evolution of the transmission signal (orange) in response to the two-step pulse sequence (blue). The Raman detuning is null. The pink zone in the inset shows the 1 μ s-long detection window. The 150 μ s-long second pulse is stopped when the transmission signal reaches a steady-state value.

mm diameter and 1.4 mm long chamber. The cell is heated to 82°C in a physics package covered by a single-layer mu-metal shield. A static magnetic field of about 250 mG is applied to raise the Zeeman degeneracy. The light transmitted through the cell is detected by a photodiode (Thorlabs PDA36A2). The output signal of the photodiode is employed in two servo loops. The first one stabilizes the laser frequency onto the bottom of the absorption line of interest using synchronous modulation-demodulation of the laser current with a lock-in amplifier. The second loop is used for stabilization of the LO frequency. In this loop, the photodiode output is sent to an analog circuit, that offsets and amplifies the signal, in order to benefit from the full dynamic range of the analog to digital converter (ADC) used to digitize the atomic signal.

Figure 1(b) shows the Ramsey-like sequence. It is composed of two-step pulses separated by a dark time $T^{26,28}$. In

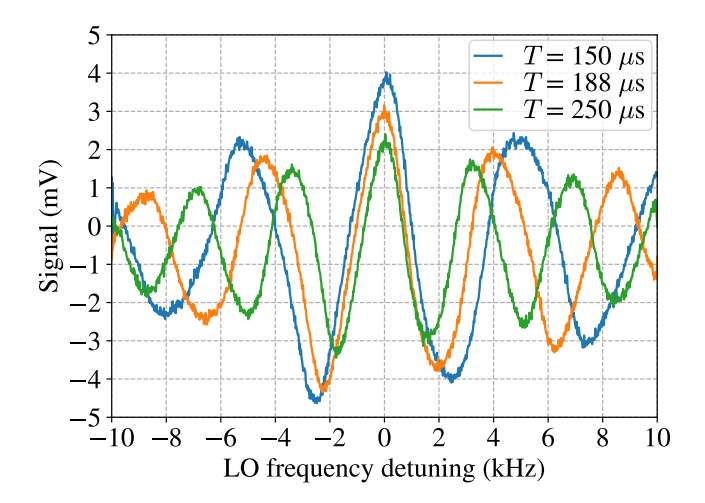


FIG. 3: Ramsey-CPT fringes detected in a Cs-Ne cell using the two-step pulse Ramsey-CPT sequence, for three different values of the dark time T (150, 188 and 250 μ s). Other parameters of the sequence are: $\tau_1 = 20 \ \mu$ s, $\tau_2 = 150 \ \mu$ s, $\tau_d = 18 \ \mu$ s, $\tau_D = 1 \ \mu$ s. The laser power P_l is 180 μ W. For each spectrum, a dc background level was subtracted from the data.

the first stage of the pulse, the laser dc current is briefly tuned, for a length τ_1 , at the high value I_1 such that the VCSEL thermal transient is accelerated and the desired optical frequency (F' = 4 state) is crossed after 10 to 20 μ s. In the second stage, of length τ_2 , the laser dc current is kept at the value I_2 so that the diode's junction cools down and the laser frequency is resonant with the desired line for a relatively long duration. The experiment is managed by a Red Pitaya STEMlab 125-14 board. This board is based on the Xilinx Zyng 7010 SoC architecture. The Zyng system combines a field programmable gate array (FPGA) with an ARM processor running a Linuxbased operating system. The board includes two analog inputs (14-bit ADC) and two analog outputs (14-bit DAC) directly connected to the FPGA and clocked at 125 MHz³³. The FPGA implements the real time programmable logic (PL) required for the Ramsey sequence generation and atomic signal processing, as well as the real time feedback in closed loop operation of the clock. The Linux processing system (PS) handles the configuration parameters for the PL, the data storage and the communication with the graphical user interface (GUI), implemented in a personal computer (PC). The two analog outputs of the Red Pitaya respectively control the VC-SEL diode current modulation and the frequency modulation of the 4.596 GHz signal. The first analog input is used to measure the cell transmission signal. Due to the nature of the direct modulation scheme, a careful synchronization of the observation window and the current pulses is critical. The detection window length τ_D and delay time τ_d , as shown on Fig. 1(b), are manually fine tuned in the PC GUI and managed by the PL in the Red Pitaya board by means of a Look-Up Table (LUT).

The LO frequency servo loop is fully managed by the PL system. In closed-loop operation, square wave modulation of the LO frequency is performed to scan both sides of the cen-

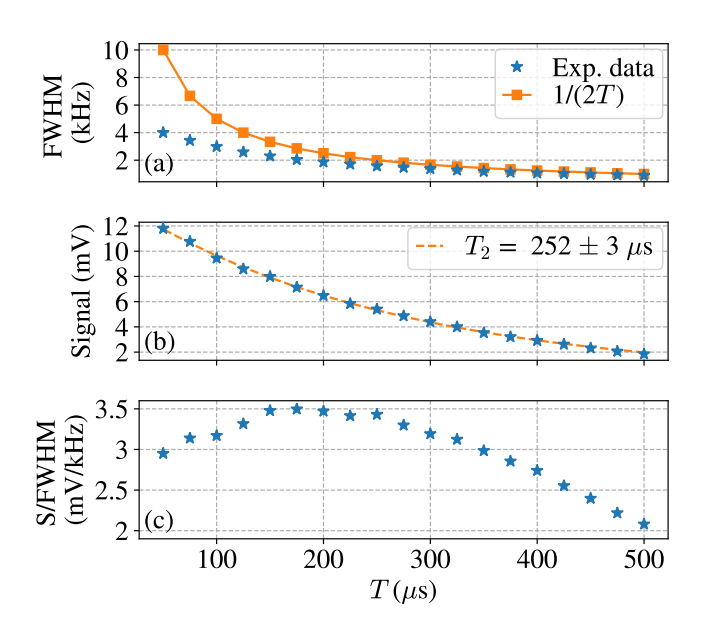


FIG. 4: FWHM, signal and signal/FWHM of the central Ramsey-CPT fringe versus the dark time *T*. On (b), the dashed line is an exponential decay fit function to the data.

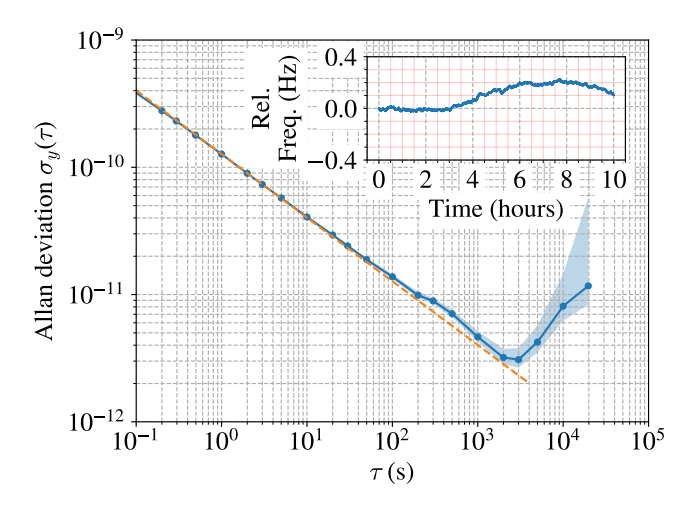
tral Ramsey fringe. An error signal, obtained by subtracting the data of two successive Ramsey cycles, is then integrated to generate a correction offset value which, added to the frequency modulation pattern, is sent by the DAC2 of the digital board to the frequency modulation input of the synthesizer.

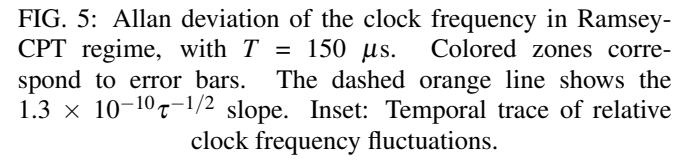
Figure 2 illustrates the transmission signal, detected at the photodiode output, in response to a typical two-step sequence. The detection window, highlighted in the inset, and fixed here to a length $\tau_D=1~\mu s$ to limit the range covered by the laser frequency, is opened after a delay $\tau_d=18~\mu s$ within the first step ($\tau_1=20~\mu s$). It is followed by the second step used for CPT pumping ($\tau_2=150~\mu s$) at the end of which atoms are resonant with the first-order sidebands, in steady-state. This stage is followed by the dark time T, set here at 150 μs .

Figure 3 shows Ramsey-CPT fringes detected in the Cs-Ne microcell using the two-step pulse Ramsey-CPT sequence, for three values of the dark time T. The total laser power P_l at the cell input is about 180 μ W. We observe that lower T values yield an increased absolute value of the light-shift^{28,34}.

Figures 4(a,b,c) respectively show the linewidth (FWHM), the signal, and the signal/FWHM of the central fringe versus T. On Fig. 4(a), we observe that the FWHM of the central fringe is narrower than the expected Ramsey 1/(2T) linewidth, for T values lower than 300 μ s. This phenomenon was already observed in Ref. 20 and is explained in 16. Figure 4(b) shows that the amplitude of the fringe is reduced with increased T due to relaxation of the atoms. By fitting the fringe signal-versus-T dependence by an exponential decay function, we extract a CPT coherence lifetime T_2 of $252 \pm 3 \mu s$. On Fig. 4(c), we note that the signal/FWHM ratio, a key figure of merit for the clock short-term stability, is maximized at a value of about 3.5 mV/kHz in the 150 - 250 μ s range.

We have performed a clock stability measurement, lasting





over 10 hours, with parameters $T = 150 \mu s$, $\tau_1 = 20 \mu s$, $\tau_2 = 150 \ \mu \text{s}$ and a laser power $P_l = 180 \ \mu \text{W}$. The results are shown in Fig. 5. The clock short-term fractional frequency stability is $1.3 \times 10^{-10} \tau^{-1/2}$ up to 2000 s. The stability at 1 s is reasonably preserved (a factor of two worse), in comparison with the one obtained by the Ramsey-CPT microcell clock described in Ref.²⁰, with $T = 150 \mu s$, using an external AOM for the sequence generation, and is twice better than the one (3×10^{-10}) of the commercial CSAC-SA65³⁵. For $\tau > 2000$ s. we observe a degradation of the clock stability. The latter could be attributed to residual light-shifts induced by temperature variations of the setup²⁴, experienced by the atoms during the optical pulses of the Ramsey-CPT sequence²⁰, or arising from the fact that the detection time could evolve a little and then be performed at slightly different laser wavelengths along the repetitive sequence cycles²⁸. At 1 day, the clock stability might be also limited by Ne gas permeation through the borosilicate glass windows of the cell. In previous studies, this effect was found to limit the stability of Cs-Ne microcell clocks at a level of a few 10^{-11} at 10^5 s^{24,36,37}. The stability obtained in this work should be of the same order at 1 day.

An expected advantage of Ramsey spectroscopy, in comparison with the CW-regime, is to mitigate the sensitivity of the clock frequency to variations of the light-field parameters, among which the laser power is an important contributor. Through routine measurements of the clock frequency and by applying laser power changes using the NDF placed at the cell input, we extracted two light-shift curves, reported in Fig. 6, obtained in the CW-regime and Ramsey ($T = 150 \mu s$) cases. These tests were done with identical physical experimental conditions and the same LO modulation frequency. In both regimes, a non-linear light-shift trend is obtained, with reduction of the light-shift sensitivity at higher laser power values. In the Ramsey case, we obtain a sensitivity of about 0.7 Hz/ μ W, i.e. 23.2 Hz/(mW/cm²), around the set-point

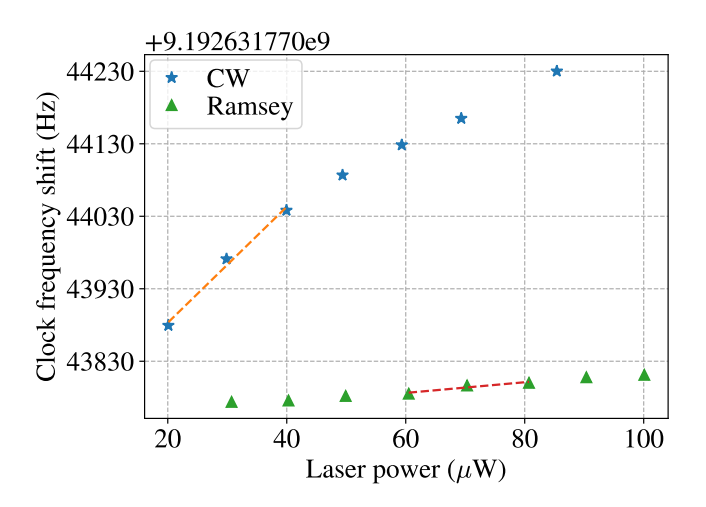


FIG. 6: Clock frequency shift, relative to the unperturbed Cs atom frequency (indicated on the top), versus the laser power, using the two-step pulse Ramsey-CPT interrogation sequence $(T = 150 \ \mu s)$, in comparison to the CW-regime. Dashed lines are local linear fits to the data.

of 70 μ W. In the CW case, the coefficient measured in the 20 - 40 μ W power range, where the short-term stability is optimized²⁰, is 8 Hz/ μ W, (251.2 Hz/(mW/cm²)), i.e. more than ten times higher than for the Ramsey case.

In conclusion, we have demonstrated operation of a microwave microcell atomic clock in the pulsed Ramsey-CPT regime by directly driving, with a sequence made of twostep pulses separated by a free-evolution dark time, the current of a VCSEL. This experiment, managed by a FPGAbased digital board and without any external optical modulator, yielded the detection of narrow and high-contrast Ramsey-CPT fringes. A microcell CPT atomic clock with an instability of $1.3 \times 10^{-10}/\sqrt{\tau}$ up to 2000 s was demonstrated, with a dark time $T = 150 \mu s$. The power light-shift coefficient, measured with $T = 150 \mu s$, was found to be about 10 times lower than the one measured in the CW regime. In the future, we plan to explore, with direct driving current modulation of the VCSEL, the application of the SABR sequence^{22,23} for further light-shift mitigation, in combination with the use of a micromachined cell built with alumino-silicate glass (ASG) for mitigation of Ne permeation^{24,37}. These efforts might pave the way to the demonstration of fully-integrated Ramsey-CPT microcell clocks with enhanced long-term stability.

This work was supported by the Direction Générale de l'Armement (DGA) and by the Agence Nationale de la Recherche (ANR) in the frame of the ASTRID project named PULSACION (Grant ANR-19-ASTR-0013-01), LabeX FIRST-TF (Grant ANR 10-LABX-48-01), EquipX Oscillator-IMP (Grant ANR 11-EQPX-0033) and EIPHI Graduate school (Grant ANR-17-EURE-0002). The PhD thesis of C.Rivera is co-funded by the program FRANCE2030 QuanTEdu (Grant ANR-22-CMAS-0001) and Centre National d'Etudes Spatiales (CNES). This work was supported by the french RENATECH network and its FEMTO-ST technological facility (MIMENTO).

DATA AVAILABILITY STATEMENT

The data supporting the findings of this study are available from the corresponding author upon reasonable request.

CONFLICT OF INTEREST

The authors state that there is no conflict of interest to disclose.

- ¹J. Kitching, "Chip-scale atomic devices," Appl. Phys. Rev. 5, 031302 (2018).
- ²J. Kitching, S. Knappe, and L. Hollberg, "Miniature vapor-cell atomic-frequency references," Appl. Phys. Lett. **81**, 3, 553–555 (2002).
- ³S. Knappe, V. Gerginov, P. D. D. Schwindt, V. Shah, H. G. Robinson, L. Hollberg, and J. Kitching, "Atomic vapor cells for chip-scale atomic clocks with improved long-term frequency stability," Opt. Lett. **30**, 18, 2351–2353 (2005).
- ⁴A. Douahi, L. Nieradko, J.-C. Beugnot, J. A. Dziuban, H. Maillote, S. Guérandel, M. Moraja, C. Gorecki, and V. Giordano, "Vapour microcell for chip scale atomic frequency standard," Elec. Lett. 43, 5, 279–280 (2007).
- ⁵S. Karlen, J. Gobet, T. Overstolz, J. Haesler, and S. Lecomte, "Lifetime assessment of RbN₃-filled MEMS atomic vapor cells with Al₂O₃ coating," Opt. Express **25**, 3, 2187–2194 (2017).
- ⁶C. Affolderbach, A. Nagel, S. Knappe, C. Jung, D. Wiedenmann, and R. Wynands, "Nonlinear spectroscopy with a vertical-cavity surfaceemitting laser (VCSEL)," Appl. Phys. B 70, 407–413 (2000).
- ⁷R. Vicarini, M. Abdel Hafiz, V. Maurice, N. Passilly, E. Kroemer, L. Ribetto, V. Gaff, C. Gorecki, S. Galliou, and R. Boudot, "Mitigation of temperature-induced light-shift effects in miniaturized atomic clocks," IEEE Trans. Ultrason. Ferroelec. Freq. Contr. 66, 12, 1962–1967 (2019).
- ⁸M. Zhu and L. S. Cutler, "Theoretical and experimental study of light shift in a cpt-based rb vapor cell frequency standard," 32nd Annual Precise Time and Time Interval (PTTI) Meeting, 311–323 (2000).
- ⁹V. Shah, V. Gerginov, P. D. D. Schwindt, S. Knappe, L. Hollberg, and J. Kitching, "Continuous light-shift correction in modulated coherent population trapping clocks," Appl. Phys. Lett. 89, 151124 (2006).
- ¹⁰R. Lutwak, A. Rashed, M. Varghese, G. Tepolt, M. M. J. LeBlanc, D. K. Serkland, K. M. Geib, G. M. Peake, and S. Romisch, "The chip-scale atomic clock prototype evaluation," in Proceeding of Precise Time and Time Interval (PTTI) Meeting, 269–290 (2007).
- ¹¹Y. Zhang, W. Yang, S. Zhang, and J. Zhao, "Rubidium chip-scale atomic clock with improved long-term stability through light intensity optimization and compensation for laser frequency detuning," J. Opt. Soc. Am. B 33, 8, 1756–1763 (2016).
- ¹²S. Yanagimachi, K. Harasaka, R. Suzuki, M. Suzuki, and S. Goka, "Reducing frequency drift caused by light shift in coherent population trapping-based low-power atomic clocks," Appl. Phys. Lett. 116, 104102 (2020).
- ¹³D. Miletic, C. Affolderbach, M. Hasegawa, R. Boudot, C. Gorecki, and G. Mileti, "AC stark-shift in CPT-based Cs miniature atomic clocks," Appl. Phys. B **109**, 89–97 (2012).
- ¹⁴ V. Yudin, M. Y. Basalaev, A. V. Taichenachev, J. W. Pollock, Z. L. Newman, M. Shuker, A. Hansen, M. T. Hummon, R. Boudot, E. A. Donley, and J. Kitching, "General methods for suppressing the light-shift in atomic clocks using power modulation," Phys. Rev. Appl. 14, 024001 (2020).
- ¹⁵M. Abdel Hafiz, R. Vicarini, N. Passilly, C. E. Calosso, V. Maurice, J. Pollock, A. Taichenachev, V. I. .Yudin, J. Kitching, and R. Boudot, "Protocol for light-shift compensation in a continuous-wave microcell atomic clock," Phys. Rev. Appl. 14, 034015 (2020).
- ¹⁶M. Abdel Hafiz, G. Coget, P. Yun, S. Guérandel, E. de Clercq, and R. Boudot, "A high-performance Raman-Ramsey Cs vapor cell atomic clock," J. Appl. Phys. **121**, 104903 (2017).
- ¹⁷X. Liu, V. I. Yudin, A. V. Taichenachev, J. Kitching, and E. A. Donley, "High contrast dark resonances in a cold-atom clock probed with counterpropagating circularly polarized beams," Appl. Phys. Lett. **111**, 224102 (2017).

- ¹⁸R. Elvin, G. W. Hoth, M. Wright, B. Lewis, J. P. McGilligan, A. S. Arnold, P. F. Griffin, and E. Riis, "Cold-atom clock based on a diffractive optic," Opt. Express 27, 26, 38359–38366 (2019).
- ¹⁹R. Boudot, V. Maurice, C. Gorecki, and E. de Clercq, "Pulsed coherent population trapping spectroscopy in microfabricated Cs–Ne vapor cells," J. Opt. Soc. Am. B 35, 5, 1004–1010 (2018).
- ²⁰C. Carlé, M. Petersen, N. Passilly, M. Abdel Hafiz, E. de Clercq, and R. Boudot, "Exploring the use of Ramsey-CPT spectroscopy for a microcell-based atomic clock," IEEE Trans. Ultrason. Ferroelec. Freq. Contr. 68, 10, 3249–3256 (2021).
- ²¹M. Abdel Hafiz, G. Coget, M. Petersen, C. Rocher, S. Guérandel, T. Zanon-Willette, E. de Clercq, and R. Boudot, "Toward a high-stability coherent population trapping Cs cell atomic clock using Auto-Balanced Ramsey spectroscopy," Phys. Rev. Appl. 9, 064002 (2018).
- ²²M. Abdel Hafiz, G. Coget, M. Petersen, C. E. Calosso, S. Guérandel, E. de Clercq, and R. Boudot, "Symmetric autobalanced Ramsey interrogation for high-performance coherent-population-trapping vapor-cell atomic clock," Appl. Phys. Lett. 112, 244102 (2018).
- ²³M. Abdel Hafiz, C. Carlé, N. Passilly, J.-M. Danet, C. E. Calosso, and R. Boudot, "Light-shift mitigation in a microcell-based atomic clock with symmetric auto-balanced Ramsey spectroscopy," Appl. Phys. Lett. 120, 064101 (2022).
- ²⁴C. Carlé, M. Abdel Hafiz, S. Keshavarzi, R. Vicarini, N. Passilly, and R. Boudot, "Pulsed-CPT Cs-Ne microcell atomic clock with frequency stability below 2×10⁻¹² at 10⁵ s," Opt. Express 31, 5, 8160–8169 (2023).
- ²⁵J. Yang, Y. Tian, B. Tan, P. Yun, and S. Gu, "Exploring Ramsey-coherent population trapping atomic clock realized with pulsed microwave modulator laser," IEEE Trans. Instr. Meas. 115, 093109 (2014).
- ²⁶T. Ide, S. Goka, and Y. Yano, "CPT pulse excitation method based on vc-sel current modulation for miniature atomic clocks," in Proceedings of the IEEE International Frequency Control Symposium European Frequency and Time Forum Joint Meeting (2015).
- ²⁷M. Fukuoka, D. Haraguchi, and S. Goka, "Light-shift characteristics of Ramsey-coherent population trapping resonances excited by two-step drive current," International Frequency Control Symposium, 228–231 (2019).
- ²⁸M. Fukuoka, S. Goka, M. Kajita, and Y. Yano, "Light shift of Ramsey-coherent population trapping resonance using drive current modulation," Jpn. J. Appl. Phys. 62, 122005 (2023).
- ²⁹M. Fukuoka and S. Goka, "Simultaneous observation of semi-continuous and ramsey-coherent population trapping resonances using the ramsey pulse sequence with drive current modulation," Jpn. J. Appl. Phys. (2023), 10.35848/1347-4065/ad160a.
- ³⁰E. Kroemer, J. Rutkowski, V. Maurice, R. Vicarini, M. Abdel Hafiz, C. Gorecki, and R. Boudot, "Characterization of commercially vertical-cavity surface-emitting lasers tuned on Cs D₁ line at 894.6 nm for atomic clocks," Appl. Opt. 55, 31, 8839–8847 (2016).
- ³¹M. Hasegawa, R. K. Chutani, C. Gorecki, R. Boudot, P. Dziuban, V. Giordano, S. Clatot, and L. Mauri, "Microfabrication of cesium vapor cells with buffer gas for MEMS atomic clocks," Sens. Actuat. A: Phys. 167, 594–601 (2011).
- ³²R. Vicarini, V. Maurice, M. Abdel Hafiz, J. Rutkowski, C. Gorecki, N. Passilly, L. Ribetto, V. Gaff, V. Volant, S. Galliou, and R. Boudot, "Demonstration of the mass-producible feature of a Cs vapor microcell technology for miniature atomic clocks," Sens. Actuat. A: Phys. 280, 99–106 (2018).
- ³³C. E. Calosso, A. C. C. Olaya, and E. Rubiola, "Phase-noise and amplitude-noise measurement of dacs and ddss," IEEE Transact. Ultrason. Ferroelec. Freq. Control 67, 2, 431–439 (2020).
- ³⁴P. R. Hemmer, M. Shahriar, V. D. Natoli, and S. Ezekiel, "Ac stark shifts in a two-zone raman interaction," J. Opt. Soc. Am. B 6, 8, 1519–1528 (1989).
- ³⁵Microchip, "Csac microchip csac-sa65,".
- ³⁶S. Abdullah, C. Affolderbach, F. Gruet, and G. Mileti, "Aging studies on micro-fabricated alkali buffer-gas cells for miniature atomic clocks," Appl. Phys. Lett. **106**, 163505 (2015).
- ³⁷C. Carlé, S. Keshavarzi, A. Mursa, P. Karvinen, R. Chutani, S. Bargiel, S. Queste, R. Vicarini, P. Abbé, M. Abdel Hafiz, V. Maurice, R. Boudot, and N. Passilly, "Reduction of helium permeation in microfabricated cells using aluminosilicate glass substrates and Al₂O₃ coatings," J. Appl. Phys. 133, 214501 (2023).